

SAILOR: Structural Augmentation Based Tail Node Representation Learning

Jie Liao
Sun Yat-sen University
Guangzhou, China
liao27@mail2.sysu.edu.cn

Jintang Li
Sun Yat-sen University
Guangzhou, China
lijt55@mail2.sysu.edu.cn

Liang Chen*
Sun Yat-sen University
Guangzhou, China
chenliang6@mail.sysu.edu.cn

Bingzhe Wu
Tencent AI Lab
Shenzhen, China
wubingzhe@pku.edu.cn

Yatao Bian
Tencent AI Lab
Shenzhen, China
yatao.bian@gmail.com

Zibin Zheng
Sun Yat-sen University
Guangzhou, China
zhzibin@mail.sysu.edu.cn

ABSTRACT

Graph neural networks (GNNs) have achieved state-of-the-art performance in representation learning for graphs recently. However, the effectiveness of GNNs, which capitalize on the key operation of message propagation, highly depends on the quality of the topology structure. Most of the graphs in real-world scenarios follow a long-tailed distribution on their node degrees, that is, a vast majority of the nodes in the graph are *tail* nodes with only a few connected edges. GNNs produce inferior node representations for tail nodes due to the lack of sufficient structural information. In the pursuit of promoting the performance of GNNs for tail nodes, we explore how the deficiency of structural information deteriorates the performance of tail nodes and propose a general structural augmentation based tail node representation learning framework, dubbed as SAILOR, which can jointly learn to augment the graph structure and extract more informative representations for tail nodes. Extensive experiments on six public benchmark datasets demonstrate that SAILOR outperforms the state-of-the-art methods for tail node representation learning.

CCS CONCEPTS

• **Computing methodologies** → **Learning latent representations**; • **Information systems** → *Data mining*.

KEYWORDS

Graph neural networks, long-tailed degree distribution, graph representation learning

ACM Reference Format:

Jie Liao, Jintang Li, Liang Chen, Bingzhe Wu, Yatao Bian, and Zibin Zheng. 2023. SAILOR: Structural Augmentation Based Tail Node Representation

*Liang Chen is the corresponding author.

Permission to make digital or hard copies of all or part of this work for personal or classroom use is granted without fee provided that copies are not made or distributed for profit or commercial advantage and that copies bear this notice and the full citation on the first page. Copyrights for components of this work owned by others than the author(s) must be honored. Abstracting with credit is permitted. To copy otherwise, to republish, to post on servers or to redistribute to lists, requires prior specific permission and/or a fee. Request permissions from permissions@acm.org.
CIKM '23, October 21–25, 2023, Birmingham, United Kingdom
© 2023 Copyright held by the owner/author(s). Publication rights licensed to ACM.
ACM ISBN 979-8-4007-0124-5/23/10...\$15.00
<https://doi.org/10.1145/3583780.3615045>

Learning. In *Proceedings of the 32nd ACM International Conference on Information and Knowledge Management (CIKM '23)*, October 21–25, 2023, Birmingham, United Kingdom. ACM, New York, NY, USA, 11 pages. <https://doi.org/10.1145/3583780.3615045>

1 INTRODUCTION

A majority of data on the Web can be represented in the form of graphs [10, 19, 26, 32]. For example, the association between the web pages can be modeled as a citation network [27, 30] so that we can carry some network analysis [20, 28] or graph algorithms [8, 24] on them to mine meaningful information for downstream applications, ranging from grouping pages by field to recommending web pages. Among numerous graph data mining algorithms, graph neural networks (GNNs) [11, 18, 35, 37, 39] take the top spot in recent years. GNNs are superior at learning representations for graphs and have been widely used in real-world scenarios, such as community detection on social media platforms [34, 40], product recommendations on e-commerce systems [3, 25], and so forth. In particular, GNNs rely on a global message propagation mechanism, which enables nodes to recursively gather information (*i.e.*, node features like bags of words for web pages) from their neighbors. Thus, the quality of the provided topological structure has a significant impact on the performance of GNNs.

However, most graphs in real-world scenarios suffer from a severe imbalance of topology structure, *i.e.*, they follow a long-tailed distribution on their node degrees. Following previous work [22, 23, 42], we refer to the low-degree nodes as *tail nodes* and the high-degree nodes as *head nodes* in contrast. Figure 1(a) illustrates that the bulk of the graph's nodes is tail nodes. Particularly, the area of the blue block under the curve represents the total number of tail nodes, while the area of the red block beneath the curve indicates the total number of head nodes. Since tail nodes are prevalent and constitute the majority of nodes in a graph, it is essential to focus on their performance in downstream tasks. Unfortunately, most state-of-the-art GNNs do not attach special attention to tail nodes, and the deficiency in neighborhood information deteriorates their performance in learning representations for tail nodes, as demonstrated in Figure 1(b). Therefore, in this work, we aim to improve the downstream task performance of tail nodes.

Recent research [33, 38] has aimed to preserve degree-specific information for nodes to improve the performance of GNNs. And the issue of degree-related bias in graph convolutional networks

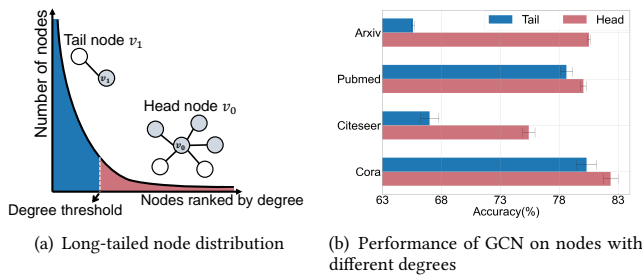


Figure 1: Illustration of long-tailed node distribution. Empirical results show that GNNs perform inferior on tail nodes.

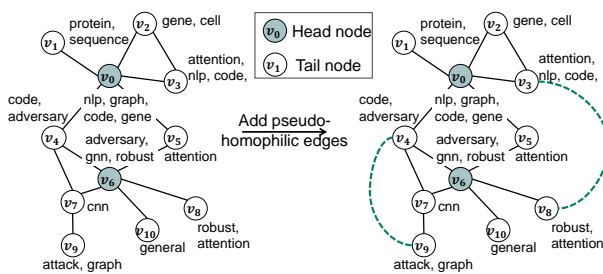


Figure 2: Illustration of adding pseudo-homophilic edges to tail nodes. More homophilic information can pass to tail nodes v_8 and v_9 via the added edges, which are presented as green dashed lines.

was first identified in [33]. The most recent work [36] aims to alleviate structural unfairness and narrow the performance gap among nodes with different degrees. However, none of these studies explicitly focus on improving representation learning for tail nodes. More closely related studies [22, 23] have formalized the long-tail problem on node degrees, that is, GNNs perform poorly on tail nodes (i.e., small-degree nodes), which make up the majority of nodes in a graph. Both studies focus on improving tail node embeddings by identifying a shared neighborhood translation pattern among all nodes. However, neither investigates the reason why a shortage of neighborhood knowledge causes tail nodes to perform worse. These works [22, 23] also introduce a setting where all head nodes are used for training and tail nodes for validation and testing. This is practical because tail nodes often have limited ground-truth label information in real-world scenarios. For example, an influencer’s occupation or gender is widely known and reliable, while that of a Twitter user with only a few followers may be uncertain. The following state-of-the-art method [42] leverages learning different feature transformation parameters, called *structural embedding* in the work, for nodes with different degrees. In this work, we follow [22, 23, 42] and target the improvement of tail node representation learning. The key difference between previous work and SAILOR is that we investigate how a shortage of structural information impairs the representation learning of tail nodes and propose to improve it from the perspective of feature diffusion.

Specifically, we investigated the distribution of homophily among head and tail nodes. In this work, *homophily* describes the phenomenon that connected nodes in the graph tend to share the same label. We discovered that due to the scarcity of neighbors, tail nodes are more likely to exhibit *total-heterophily*, meaning they do not share any labels with all their neighbors. This finding is validated both theoretically and experimentally in Section 4. We propose that the lack of structural information leads to a deficiency of homophilic neighbors for tail nodes, which can hinder the effectiveness of the GNN’s message propagation mechanism.

Furthermore, it is known that GNNs propagate messages between neighboring nodes in each layer through two separate steps: feature diffusion and feature transformation. While both head and tail nodes undergo the same feature transformation process with unified parameters, they aggregate different messages during the feature diffusion process. Existing studies on tail node representation learning [22, 23, 42] have focused on enhancing tail node embedding from the perspective of feature transformation. However, they have overlooked the inherent deficiency of homophilic neighbors for tail nodes in terms of feature diffusion caused by the lack of structural information.

These observations motivate us to develop an effective tail structure augmentor that adds *pseudo-homophilic edges*. This reduces their total heterophily and improves the performance of GNNs for tail nodes from the feature diffusion aspect. By *homophilic edge*, we mean an edge that connects two nodes with the same label. And we refer to the predicted homophilic edge by the augmentor as *pseudo-homophilic edges*. As illustrated in Figure 2, the pseudo-homophilic edges added to tail nodes v_9 and v_8 facilitate them to aggregate more homophily information from their direct surroundings and thus benefit the message-passing process.

The key challenge for the tail structure augmentor is *how to locate the pseudo-homophilic edges for tail nodes without knowing the ground-truth labels*. Furthermore, the developed model is expected to be versatile and applicable to various GNNs. To address these challenges, we propose SAILOR, a general structural augmentation based tail node representation learning framework, which jointly augments the structure for tail nodes and trains a GNN. In summary, we make the following contributions:

- We explore how the deficiency of structural information impairs the representation learning of tail nodes.
- We propose a general framework, SAILOR, that hinges on the key operation of adding pseudo-homophily edges to tail nodes to enable them to gain more task-relevant information from their immediate neighborhoods.
- We conduct extensive experiments on six public datasets and show that our proposed SAILOR outperforms state-of-the-art baselines on tail node representation learning.

2 RELATED WORK

2.1 Graph Representation Learning

Graph neural networks. Recent years have witnessed graph neural networks (GNNs) emerge as the most widely used methods for graph representation learning. Assuming connected nodes tend to share similar attributes with each other, they [4, 11, 17, 18, 35, 37, 39] usually follow a neighborhood aggregation scheme that enables

each node to receive relevant neighborhood information and update its own representation. Node classification is widely applied as the downstream task to assess the quality of the learned node representations. Nevertheless, most state-of-the-art GNNs do not attach special attention to tail nodes and perform inferior on them.

Graph data augmentation. Generally, graph data augmentation aims to obtain an optimal graph structure. Existing techniques can be categorized into three folds: feature-wise augmentation, structure-wise augmentation, and label-wise augmentation [6]. Most relevant to our work is the literature devoted to augmenting the graph structure to obtain ideal connectivity. Among these works, [1, 41] employ specific strategies to eliminate noisy edges and introduce beneficial ones to attain an optimal graph structure. [15] devotes to obtaining a clean graph from a poisoned graph and defending against types of graph adversarial attacks [2, 21]. However, our work focuses on a different problem, which is to enhance the representation learning for tail nodes.

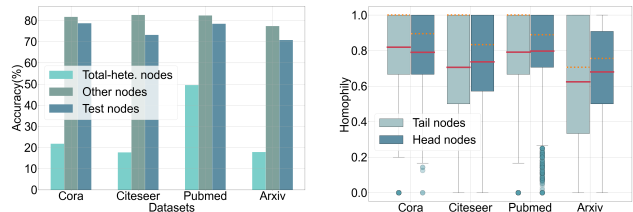
2.2 Tail Node Representation Learning

Recent research [33, 38] has aimed to preserve degree-specific information for nodes with varying degrees to improve the performance of GNNs. Specifically, DEMO-Net [38] employs a multi-task graph convolutional network to attain degree-specific embeddings for each node. Following DEMO-Net [38], SL-DSGCN [33] first explicitly points out the degree-bias issue and proposes the use of Bayesian neural networks to generate uncertainty scores for pseudo labels of unlabeled nodes, allowing for dynamic weighting of the training step size. These models aim to improve the overall performance of GNNs and do not specifically enhance the learning of tail node representations. The most recent work [36] claims that graph contrastive learning can mitigate structural unfairness and develops a graph contrastive learning-based model called GRADE. While GRADE [36] aims to narrow the performance gap among nodes with different degrees and does not focus on boosting the representation learning for tail nodes, it fails to achieve competitive performance under the setting in [22, 23].

Meta-tail2vec [23] proposes to treat the representation learning of each tail node as a meta-testing task and to construct the learning of head nodes as meta-training tasks. Similarly, TailGNN [22] aims to learn the translation pattern from a node to its neighborhood using tailored strategies. This allows the proposed model to recover missing neighborhood information for tail nodes. Cold Brew [42] employs a teacher-student distillation approach, using a GNN as the teacher model and a multi-layer perceptron (MLP) as the student model. It leverages node-wise structural embedding and a distillation scheme to complement missing neighborhood information for tail nodes. In summary, all of these works provide innovative and effective strategies for enhancing tail node representation from the feature transformation aspect. However, in terms of feature diffusion, they fail to consider the impact of the lack of structural information on the deficiency of homophilic neighbors for tail nodes.

3 PRELIMINARIES

Notation of graph. Let $G = (A, X)$ be an undirected and un-weighted graph, where $A \in \{0, 1\}^{N \times N}$ is the adjacency matrix



(a) Comparison of performance on total-heterophilic nodes versus other nodes.

(b) Homophily distribution.

Figure 3: Illustration of heterophily of tail nodes.

of the graph and $X \in \mathbb{R}^{N \times F}$ denotes F -dimension feature vectors for all N nodes. Specifically, each entry A_{ij} indicates whether the node i is connected to node j , with a value of 1 representing a connection and 0 otherwise. Additionally, the graph can also be represented as $G = (\mathcal{V}, \mathcal{E})$, where \mathcal{V} denotes the set of nodes in the graph and \mathcal{E} represents the set of edges.

Division of head and tail nodes. Following the Pareto principle [31], we first sort all nodes in ascending order according to their degrees. We then select the top 80% of nodes as tail nodes, denoted as \mathcal{V}_{tail} , and the remaining nodes as head nodes, denoted as \mathcal{V}_{head} . In practice, we calculate the total number of tail nodes while retrieving the degrees in ascending order. If the current number of tail nodes exceeds 80% of all nodes, we stop retrieving and set the corresponding degree as the degree threshold.

Problem Formulation. Given a graph $G = (A, X)$, the goal of node representation learning is to identify a function $g: A, X \rightarrow Z$ that maps each node to a low-dimensional vector. $Z \in \mathbb{R}^{N \times d}$ denotes the output embedding matrix of all nodes, where d is the dimension of the embedding vectors. In a node classification task, d is often set to C , which corresponds to the number of node classes in the given dataset. In this paper, our focus is on improving the quality of tail node representations, that is, $\{Z_v | v \in \mathcal{V}_{tail}\}$.

4 THE HETEROPHILY OF TAIL NODES

We notice that while nodes aggregate different messages during the feature diffusion process, they all share the same feature transformation process with unified model parameters. For instance, head nodes have more neighbors than tail nodes, allowing them to gather more information from their immediate surroundings. This could be a contributing factor to why GNNs perform less effectively on tail nodes than on head nodes.

Recent works [5, 13, 43] have shown that the homophily of the underlying graph, which permits nodes to obtain more task-relevant information from neighbors, has a significant impact on the performance of GNNs [11, 18, 35, 39]. In other words, if a node shares no labels with any of its neighbors, GNNs will fail to learn high-quality representation for it because it completely violates the homophily assumption. We call this kind of nodes total-heterophilic nodes in this work. We present the average node classification accuracy of a 2-layer GCN [18] on total-heterophilic nodes in Figure 3(a), and the results are in line with our expectation. It demonstrates that the performance of GNNs on total-heterophilic nodes is far inferior to other nodes in the test set.

Assuming that node labels are randomly and uniformly distributed, the probability of a head node becoming a total-heterophilic node (denoted as \mathcal{P}_h) is significantly lower than that of a tail node (denoted as \mathcal{P}_t). Formally, given that D_h and D_t represent the degree of a head and tail node respectively, \mathcal{P}_h can be expressed as $(\frac{C-1}{C})^{D_h}$, while \mathcal{P}_t is $(\frac{C-1}{C})^{D_t}$. Since D_h is much greater than D_t , it follows that \mathcal{P}_h is significantly lower than \mathcal{P}_t . This suggests that in a homophily graph, head nodes can gather more homophilic information from their direct neighbors to enhance their learned representations. In contrast, tail nodes are more likely to suffer from a lack of homophilic neighbors or even total-heterophily due to their limited number of neighbors, resulting in poorer performance than head nodes. To verify this hypothesis, we examine the homophily of head and tail nodes in detail.

We calculate the homophily [29] for each head node and tail node individually and present the results in Figure 3(b). Specifically, the red solid line represents the mean homophily of tail nodes and head nodes across four public datasets. The orange dotted line indicates the median homophily value, while the light-blue dots denote outliers. The color intensity of the dots in Figure 3(b) corresponds to the number of outliers, with a higher number of outliers resulting in a darker dot color. As shown in Figure 3(b), the average homophily of head nodes is higher than that of tail nodes in three datasets: Citeseer, Pubmed, and Arxiv. Although the node homophily of tail nodes is higher in Cora, they still suffer from more severe total-heterophily than head nodes, which has a greater impact on their inferior downstream-task performance. In addition, Figure 3(b) also indicates that tail nodes have more heterophilic neighbors in two ways: in the Citeseer, Pubmed, and Arxiv datasets, the box for tail nodes is longer, meaning that the lower quartile homophily is lower; in the Cora and Pubmed datasets, tail nodes have a higher number of total-heterophilic neighbors.

To better illustrate the difference in the proportion of total-heterophilic nodes between head and tail nodes, we provide Table 1. From Table 1, we can make two observations. Firstly, the majority of total-heterophilic nodes in the graph are tail nodes. For instance, out of the 147 total-heterophilic nodes in Cora, 143 are tail nodes. Secondly, the proportion of total-heterophilic nodes in tail nodes is significantly greater than that in head nodes. In Cora, for instance, 6.89% of tail nodes are total-heterophilic, compared to only 0.97% of head nodes. These findings suggest that tail nodes aggregate lower-quality information during the neighborhood aggregation process compared to head nodes, due to the higher proportion of total-heterophilic nodes. This introduces noise into the training of model parameters, resulting in an inferior performance of GNNs for these nodes. This motivates us to develop a model that can enhance the structural information for tail nodes and improve the performance of GNNs for these nodes.

5 THE PROPOSED FRAMEWORK: SAILOR

In this section, we present a detailed description of our proposed framework, SAILOR. The key idea behind SAILOR is the use of a tail structure augmentor to add pseudo-homophilic edges to each tail node. This allows tail nodes to aggregate more task-relevant information from their neighborhoods. By utilizing the augmented graph as input for training, the GNN can learn parameters that

Table 1: The amount and proportion of total-heterophilic nodes in head nodes, tail nodes, respectively.

		Cora	Citeseer	Pubmed	Arxiv
Head	amount	4	16	50	331
	proportion	0.97%	4.78%	1.38%	1.00%
Tail	amount	143	308	2,471	20,468
	proportion	6.89%	17.25%	15.37%	15.01%

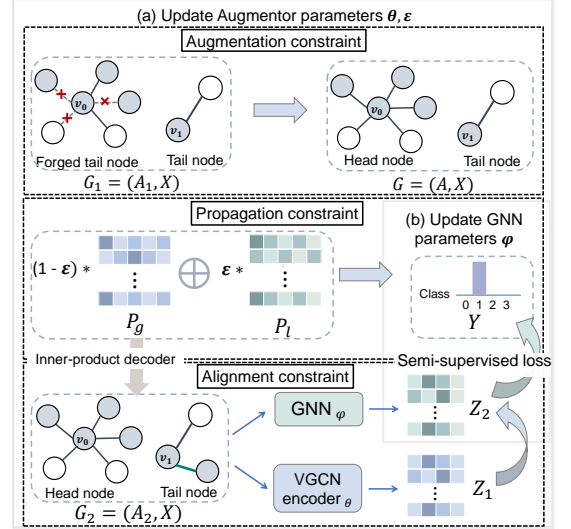


Figure 4: Overview of SAILOR, which exploits a tail structure augmentor to add pseudo-homophilic edges to each tail node. This allows tail nodes to aggregate more homophilic information from their immediate neighborhoods. By utilizing the augmented graph G_2 as input for training, the GNN can learn parameters that more accurately reflect the actual feature transformation pattern.

more accurately fit the actual feature transformation pattern. As illustrated in Figure 4, SAILOR consists of two main components: the Tail Structure Augmentor (Augmentor) and the Graph Neural Network (GNN). (a) The Augmentor is trained with the augmentation, propagation, and alignment loss to update its parameters and generates an augmented graph G_2 . (b) The GNN takes G_2 as input and is trained using a semi-supervised loss to update its feature transformation parameters ϕ . It learns node embeddings Z_2 to fine-tune the Augmentor’s parameters θ under the constraint of the alignment loss. As a result, these two components can enhance each other and be trained jointly.

5.1 Graph Neural Networks

GNNs rely on a message propagation mechanism to recursively update node representations. This mechanism drives the performance of GNNs to be highly dependent on the homophily of the underlying graph. In particular, GNNs propagate messages between neighboring nodes in each layer, which can be regarded as two separate

steps. Firstly, every node aggregates features from its neighborhood and we call this step *feature diffusion*. Mathematically,

$$\hat{H}^{(l)} = AH^{(l)}, \quad (1)$$

where $H^{(l)}$ denotes the hidden representations of the graph at the l -th layer and the initial $H^{(0)}$ is the node feature matrix X . In fact, the aggregation scheme can vary across different GNNs [11, 18, 35, 39], such as mean pooling and max pooling. Besides, the adjacent matrix can also be normalized as $\tilde{A} = \hat{D}^{-\frac{1}{2}} \hat{A} \hat{D}^{-\frac{1}{2}}$, where $\hat{A} = A + I$ and \hat{D} is the degree matrix of \hat{A} . For illustration purposes, we use Eq. (1), which is just one example that essentially employs sum pooling.

Subsequently, all nodes transform their aggregated representations with unifying model parameters ϕ . This step can be referred to as *feature transformation*. Formally,

$$H^{(l+1)} = g_{\phi}^{(l)}(\hat{H}^{(l)}) = \sigma(\hat{H}^{(l)} W_{\phi}^{(l)}), \quad (2)$$

where $W_{\phi}^{(l)}$ denotes the trainable parameters at layer l and σ is the nonlinear activation function. We take Eq. (2) for the convenience of illustration. In fact, the transformation form can vary. For example, it can also be written as $g_{\phi}^{(l)}(\hat{H}^{(l)}) = \hat{H}^{(l)} W_{\phi}^{(l)} + b_{\phi}^{(l)}$, where $b_{\phi}^{(l)}$ are learnable parameters.

It is now evident that both head and tail nodes follow the same feature transformation pattern with unified model parameters, as shown in Eq. (2). However, they aggregate different information during the feature diffusion process, as shown in Eq. (1). As discussed in Section 4, the performance of tail nodes deteriorates due to a lack of sufficient homophilic neighbors for training.

Thus, our proposed framework SAILOR trains the GNN with the augmented graph $G_2 = (A_2, X)$ which is generated by a tail structure augmentor. Since there are fewer total-heterophilic tail nodes in the augmented graph, it can facilitate the training of the GNN. The above process can be formulated as follows:

$$\begin{aligned} \hat{Z}_2^{(l)} &= A_2 Z_2^{(l)}, \\ Z_2^{(l+1)} &= g_{\phi}^{(l)}(\hat{Z}_2^{(l)}) = \sigma(\hat{Z}_2^{(l)} W_{\phi}^{(l)}), \end{aligned} \quad (3)$$

where σ is the activation function, $\phi = \{W_{\phi}^{(l)} \mid l \in \{0, 1, 2, \dots, L_2 - 1\}\}$ are trainable parameters, and L_2 is the total amount of layers of the GNN. When $l = 0$, the hidden representation is initialized by X , i.e., $Z_2^{(0)} = X$. Besides, we refer to the output of the last layer as Z_2 .

Following common practice, we train the GNN with the semi-supervised loss, which is expressed as follows:

$$\mathcal{L}_{sup} = \text{CE}(Z_2, Y), \quad (4)$$

where $\text{CE}(\cdot)$ is the cross-entropy function and Y represents the ground-truth labels of nodes in the training set.

5.2 Tail Structure Augmentor

As suggested by previous work [16, 17], learning the distribution of hidden embeddings instead of learning individual hidden embeddings can help train more robust parameters. Therefore, we deploy a Variational Graph Convolution Network (VGCN) based encoder with learnable parameters θ as the backbone architecture for the tail structure augmentor. Moreover, we design three constraint strategies to optimize the augmentor.

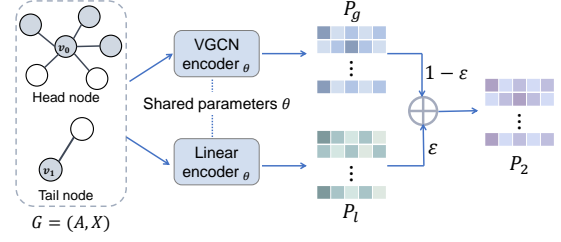


Figure 5: The VGCN encoder and linear encoder share the same feature transformation parameters θ . In contrast to the VGCN encoder, the linear encoder does not perform message propagation on nodes but instead only performs feature transformation. ϵ are trainable parameters that adaptively adjust the importance of the graph structure.

Augmentation constraint. Since the Variational Graph Auto-Encoder (VGAE) [17] is commonly used for link prediction, one might presume that it could be directly adopted to add edges for tail nodes. However, this intuitive solution is not feasible and does not perform well due to two challenges. Firstly, directly using VGAE for neighbor generation can make the model lazy as its optimal situation is to recover the original structure. In this case, the inferior performance of tail nodes remains. Secondly, in view that there are heterophilic edges in the original graph structure, this direct approach may introduce noise to the node classification task.

Towards the challenges, we propose to go beyond VGAE by training a mapping function from forged tail nodes to head nodes, allowing us to learn how to map tail nodes to structurally augmented tail nodes. Specifically, we randomly drop edges for each head node and turn them into forged tail nodes, inspired by Tail-GNN [22]. In this work, we utilize the forged tail nodes for training to replicate the circumstance of insufficient neighborhood information, which can also help mitigate the degree distribution shift problem from the training set to the test set under the dataset partitioning setting in [22, 23]. In contrast, Tail-GNN follows the idea of GAN (Generative Adversarial Nets) [9] and exploits the forged tail nodes to train a smarter discriminator.

Formally, given the original graph $G = (A, X)$, we randomly drop a certain proportion, called Δ , of edges for each head node and get a new adjacency matrix A_1 . It is evident that the original graph G is denser than $G_1 = (A_1, X)$, in which even the head nodes may lack sufficient neighborhood information. With $G_1 = (A_1, X)$ as input, the VGCN encoder $f_{\theta}(\cdot)$ conducts neighborhood aggregation for each node at each layer. It can be formulated as:

$$P_1^{(l+1)} = f_{\theta}^{(l)}(A_1, P_1^{(l)}) = \sigma(A_1 P_1^{(l)} W_{\theta}^{(l)}), \quad (5)$$

where $W_{\theta}^{(l)}$ are trainable parameters of the VGCN encoder at layer l , $P_1^{(l)}$ represents the hidden representations at layer l , $P_1^{(0)}$ is the input feature matrix X , and σ denotes the activation function.

Furthermore, we use $f_{\theta_{\mu}}(\cdot)$ and $f_{\theta_{\sigma}}(\cdot)$ to transform the output representations of the last hidden layer into the mean representation μ and standard deviation representation σ , respectively. By mapping node features to the entire latent space instead of a single point, the parameters ϕ become more robust and help to produce

more representative node embeddings. We then sample from the learned distribution to obtain the embeddings P_1 . To enable backward propagation of gradients during the sampling process, we employ the reparameterization trick as described in [17]. Formally,

$$\begin{aligned}\boldsymbol{\mu} &= f_{\theta_{\mu}}(P_1^{(L_1)}) = P_1^{(L_1)} W_{\theta}^{\mu}, \\ \boldsymbol{\sigma} &= f_{\theta_{\sigma}}(P_1^{(L_1)}) = P_1^{(L_1)} W_{\theta}^{\sigma}, \\ P_1 &= \boldsymbol{\mu} + \boldsymbol{\sigma} \odot \boldsymbol{\epsilon},\end{aligned}\quad (6)$$

where $\boldsymbol{\epsilon} \in \mathcal{N}(0, I)$ is the noise variable sampled from Gaussian distribution, L_1 represents the number of hidden layers of the VGCN encoder, and $\boldsymbol{\mu}, \boldsymbol{\sigma} \in \mathbb{R}^{N \times d}$.

Subsequently, we adopt the inner product and the activation function sigmoid(\cdot) to decode P_1 and obtain A'_1 . Formally,

$$A'_1 = \text{sigmoid}(P_1 P_1^T). \quad (7)$$

We expect the tail structure augmentor to restore missing edges for the forged tail nodes. As a result, the original graph structure A serves as the supervised signal for A'_1 . Moreover, we intend to reduce the Kullback Leibler (KL) divergence [12] between the distribution of embeddings P_1 and a Gaussian distribution, following [17]. In summary, the augmentation constraint objective for the tail structure augmentor can be formulated as:

$$\mathcal{L}_{aug} = \text{BCE}(A'_1, A) + \text{KL}[q(P_1|A_1, X) \| p(P_1)], \quad (8)$$

where $p(P_1) = \prod_{i=1}^N \mathcal{N}(p_i^1 | 0, I)$ is a Gaussian prior of node representations, and $q(P_1|A_1, X) = \prod_{i=1}^N \mathcal{N}(p_i^1 | \boldsymbol{\mu}, \text{diag}(\boldsymbol{\sigma}^2))$ is the learned distribution. BCE(\cdot) is the binary cross entropy function.

Propagation constraint. As observed in Section 4, even in a homophily graph, the graph structure of some nodes may be unreliable and introduce noise to the training of the GNN. To mitigate the negative impact of noisy graph structures of some nodes, we adopt a learnable parameter $\varepsilon \in \mathbb{R}^N$ to automatically adjust the importance of the graph structure for node representation learning. Specifically, we utilize both a VGCN encoder and a linear encoder on the input graph to derive embeddings P_g and P_l , respectively. It is important to note that the linear encoder shares parameters θ with the VGCN encoder. However, in contrast to the VGCN encoder, the linear encoder does not perform message passing on nodes but instead relies solely on parameters θ for feature transformation. Let $h_{\theta}(\cdot)$ denote the linear encoder, the above procedure can be formulated as:

$$\begin{aligned}P_g^{(l+1)} &= f_{\theta}^{(l)}(A, X) = \sigma(AP_g^{(l)} W_{\theta}^{(l)}), \\ P_l^{(l+1)} &= h_{\theta}^{(l)}(A, X) = h_{\theta}(X) = \sigma(P_l^{(l)} W_{\theta}^{(l)}),\end{aligned}\quad (9)$$

where $P_g^{(l)}$ and $P_l^{(l)}$ represent the hidden representations of the VGCN encoder and the linear encoder at layer l , respectively. When $l = 0$, both $P_g^{(0)}$ and $P_l^{(0)}$ are initialized as the input feature matrix X . We refer to the output of the last layer as P_g and P_l respectively.

As illustrated in Figure 5, ε serves as the importance weight of P_l , while $1 - \varepsilon$ serves as the one of P_g . Formally, we obtain P_2 as follows:

$$P_2 = \varepsilon * P_l + (1 - \varepsilon)P_g. \quad (10)$$

By adaptively adjusting the weight of the embeddings learned by the two encoders through ε , we can dynamically fine-tune the importance of the graph structure for learning node representation P_2 . The ground-truth labels of the training set serve as a supervised signal for P_2 , allowing us to optimize parameters ε and θ . This optimization process enables the augmentor to learn better parameters θ , thereby facilitating the generation of higher-quality augmented graphs. Mathematically, we formulate the propagation constraint objective for the tail structure augmentor as follows:

$$\mathcal{L}_p = \text{CE}(P_2, Y), \quad (11)$$

where CE(\cdot) is the cross-entropy function and Y represents the ground-truth labels of nodes in the training set.

Alignment constraint. To generate the augmented graph $G_2 = (A_2, X)$, the tail structure augmentor employs the inner product to decode P_2 . To identify the most likely existing edges among nodes, we apply the activation function softmax(\cdot) on each row of the decoded matrix to derive a peak distribution instead of using the activation function sigmoid(\cdot). We then adopt a Bernoulli-sampling procedure to obtain binary graph structure data, where 1 indicates an existing edge and 0 otherwise. Note that the sampled edges are the desired pseudo-homophily edges to be added to tail nodes. This process can be expressed mathematically as follows:

$$\begin{aligned}A'_2 &= \text{softmax}(P_2 P_2^T), \\ A_2 &= \text{Clamp}(\text{BernSamp}(A'_2) + A),\end{aligned}\quad (12)$$

where BernSamp(\cdot) denotes the Bernoulli-sampling procedure and Clamp(\cdot) represents a function that clamps values to $[0, 1]$.

The GNN mentioned in Section 5.1 is then trained on G_2 to obtain refined model parameters ϕ . Based on ϕ , the parameters θ of the augmentor can be further fine-tuned, which in return allows the augmentor to produce higher-quality augmented graphs. Specifically, given the augmented graph G_2 as input to the VGCN encoder $f_{\theta}(\cdot)$, it derives node representations Z_1 as follows:

$$\begin{aligned}Z_1^{(l+1)} &= f_{\theta}^{(l)}(A_2, Z_1^{(l)}) = \sigma(A_2 Z_1^{(l)} W_{\theta}^{(l)}), \quad l = 0, \dots, L_1 - 1 \\ \boldsymbol{\mu} &= f_{\theta_{\mu}}(Z_1^{(L_1)}) = Z_1^{(L_1)} W_{\theta}^{\mu}, \\ \boldsymbol{\sigma} &= f_{\theta_{\sigma}}(Z_1^{(L_1)}) = Z_1^{(L_1)} W_{\theta}^{\sigma}, \\ Z_1 &= \boldsymbol{\mu} + \boldsymbol{\sigma} \odot \boldsymbol{\epsilon}.\end{aligned}\quad (13)$$

We then exploit an alignment objective function to narrow the gap between Z_1 and Z_2 , thereby fine-tuning the parameters θ under the guidance of ϕ . Specifically, we employ KL divergence to measure the information loss from the learned distribution $r(Z_1|\theta)$ to $t(Z_2|\phi)$ and take $t(Z_2|\phi)$ as the prior. Formally,

$$\mathcal{L}_{ali} = \text{KL}[r(Z_1|\theta) \| t(Z_2|\phi)]. \quad (14)$$

5.3 Optimization of SAILOR

In summary, the overall objective function of SAILOR can be formulated as follows:

$$\begin{aligned}\arg \min_{\theta, \varepsilon, \phi} \mathcal{L} &= \mathcal{L}_{\theta, \varepsilon} + \alpha \mathcal{L}_{\phi}, \\ \text{where } \mathcal{L}_{\phi} &= \mathcal{L}_{sup}, \\ \text{and } \mathcal{L}_{\theta, \varepsilon} &= \beta \mathcal{L}_{aug} + \eta \mathcal{L}_p + \delta \mathcal{L}_{ali}.\end{aligned}\quad (15)$$

Algorithm 1: The training process of SAILOR.

Input: Graph $G = (A, X) = (\mathcal{V}, \mathcal{E})$, tail nodes \mathcal{V}_{tail} , batch size B , learning rate lr_g, lr_a

Output: GNN parameters ϕ

- 1 Initialize model parameters $\theta, \varepsilon, \phi$;
- 2 **while** *not converged* **do**
- 3 $i = 0$ and the edge set of the augmented graph $\mathcal{E}_2 = \mathcal{E}$;
 // Add pseudo-homophilic edges to tail nodes.
- 4 **while** $i < |\mathcal{V}_{tail}|$ **do**
- 5 batch = $\mathcal{V}_{tail}[i:i+B]$;
- 6 $A'_{2b} = \text{softmax}(P_2[\text{batch}] P_2^T)$;
- 7 $\mathcal{E}' = \text{Nonzero}(\text{BernSamp}(A'_{2b}))$;
- 8 $\mathcal{E}_2 = \mathcal{E}_2 \cup \mathcal{E}'$;
- 9 $i = i + B$;
- // Update the GNN.
- 10 $L_{sup} \leftarrow \text{CE}(Z_2, Y)$;
- 11 $\phi \leftarrow \phi - lr_g \frac{\partial \alpha L_{sup}}{\partial \phi}$;
- // Update the augmentor.
- 12 $L_{\theta, \varepsilon} \leftarrow \beta \mathcal{L}_{aug} + \eta \mathcal{L}_P + \delta \mathcal{L}_{ali}$;
- 13 $\theta \leftarrow \theta - lr_a \frac{\partial L_{\theta, \varepsilon}}{\partial \theta}$;
- 14 $\varepsilon \leftarrow \varepsilon - lr_a \frac{\partial L_{\theta, \varepsilon}}{\partial \varepsilon}$;
- 15 **return** ϕ

Table 2: Summary of datasets. “DegTh.” denotes the degree threshold that split the nodes into 80% tail nodes and 20% head nodes, as stated in Section 3. “#Feat.” denotes the dimension of each node feature vector.

	#Node	#Edge	#Feat.	#Class	DegTh.
Chameleon [30]	2,277	62,742	2,325	5	33
Squirrel [30]	5,201	396,706	2,089	5	123
Cora [32]	2,485	10,138	1,433	7	5
Citeseer [32]	2,120	7,358	3,703	6	5
Pubmed [32]	19,717	88,648	500	3	6
Arxiv [14]	169,343	2,315,598	128	40	17

where the predefined parameter α controls the impact of the GNN on the overall optimization process. β, η , and δ govern the relative weights of the three constraints for the tail structure augmentor. We train the tail structure augmentor and the GNN concurrently to optimize \mathcal{L} . The augmented graph G_2 is generated by the tail structure augmentor and used to train the GNN. In return, the GNN derives node representations Z_2 , which serve as the prior to fine-tune the tail structure augmentor. As a result, these two components enhance each other and are trained jointly.

To provide a clear explanation of our method, we detail the training algorithm as in Algorithm 1. Although decoding the node representations to the graph structure can lead to a space complexity of $O(N^2)$, it is easy to achieve an acceptable space complexity of $O(B^2)$ by batch-processing. Here B denotes the number of nodes in a batch. Additionally, we deploy the commonly used early-stopping mechanism to accelerate the model training and prevent overfitting.

6 EXPERIMENTS

In this section, we evaluate the effectiveness of SAILOR through comprehensive experiments. Firstly, we compare SAILOR to state-of-the-art tail node representation learning methods using two evaluation metrics on six public datasets. The results demonstrate that SAILOR outperforms the baselines. Secondly, we compare the homophily distribution of all nodes in the original graph to that in the augmented graph, which shows that the pseudo-homophilic edges are located as expected. Thirdly, we compare SAILOR with its four variants to examine the importance of different components and explore its sensitivity to different hyper-parameters. Lastly, we align the dataset partitioning setting with that of GCN [18] to further confirm the effectiveness of SAILOR and show that the performance of head nodes is not compromised by SAILOR.

6.1 Experimental Setups

Datasets and Settings. We evaluate SAILOR with a total of six benchmark datasets, as summarized in Table 2. For each dataset, we extract the largest connected component and processed edges as undirected. We follow previous work [22, 23] by using all head nodes for training and splitting the tail nodes into validation and test sets with a ratio of 1:4. All baselines are initialized with the settings provided in their respective open-source codes. We further fine-tune these settings to improve their performance. Experiments are conducted ten times using different random seeds, and we present the average results along with standard deviations. The source code is available at <https://github.com/Jie-Re/SAILOR.git>.

Baselines. We compare SAILOR with classic GNNs and state-of-the-art tail node representation learning methods, which include:

- **GCN** [18]: It is a widely used graph neural network.
- **DEMO-Net** [38]: It is a degree-aware graph neural network. We employ GCN as its base architecture.
- **Meta-tail2vec** [23]: It applies the meta-learning framework MAML [7] and learns to refine tail node embeddings.
- **Tail-GCN** [22]: It exploits an end-to-end framework to recover missing neighborhood features for tail nodes. We employ GCN as its base architecture for a fair comparison.
- **Cold Brew** [42]: It devotes to addressing the strict cold start problem. Since the MLP student of Cold Brew is inferior to the teacher GNN on tail nodes, we report the performance of the latter and employ GCN as its base architecture.
- **GRADE** [36]: It is a graph contrastive learning-based method aiming to narrow the performance gap among nodes with different degrees.

6.2 Long-tailed Node Classification

We conduct the node classification task on six public datasets to assess the effectiveness of SAILOR. We use accuracy as our evaluation metric. Additionally, previous works [22, 23] have also adopted the micro-F score as an evaluation metric. However, the micro-F score used by Tail-GNN [22] is calculated by ignoring the largest class, which differs from the standard definition. In fact, the commonly used Micro-F1 score is mathematically equivalent to accuracy when there is one ground-truth label for each data point [41]. To maintain the consideration of class imbalance in the evaluation metric of

Table 3: Evaluation of tail node classification using GCN as the base model. The best results are shown in bold and the runners-up are underlined. "OOM" denotes that the model runs out of memory.

	Metric (%)	GCN	DEMO-Net	Meta-tail2vec	Tail-GCN	Cold Brew	GRADE	SAILOR
Chameleon	Accuracy	36.66±2.27	32.23±0.86	19.08±2.57	31.06±1.21	<u>40.01±0.39</u>	33.81±0.94	40.10±0.90
	Weighted-F1	34.24±2.81	29.09±1.11	13.00±1.89	25.77±3.49	<u>37.20±0.73</u>	29.19±1.94	38.56±1.00
Squirrel	Accuracy	30.04±1.55	20.82±0.56	19.04±0.19	20.38±0.61	<u>31.75±1.02</u>	23.05±0.71	32.79±0.46
	Weighted-F1	<u>26.79±2.29</u>	16.27±0.71	9.97±0.78	13.91±0.92	26.56±1.89	18.84±0.99	27.48±1.02
Cora	Accuracy	85.16±0.49	84.43±0.72	77.58±0.48	84.27±0.79	<u>86.13±0.12</u>	82.77±0.85	86.92±0.50
	Weighted-F1	85.20±0.50	84.57±0.69	77.63±0.50	84.16±0.89	<u>86.11±0.13</u>	82.75±0.86	86.93±0.47
Citeseer	Accuracy	<u>72.06±0.48</u>	71.39±0.46	65.59±0.99	71.81±1.18	70.76±0.39	66.65±2.25	74.30±0.47
	Weighted-F1	<u>71.08±0.53</u>	70.29±0.67	63.99±1.06	70.18±1.03	69.43±0.42	64.54±1.95	72.22±0.50
Pubmed	Accuracy	<u>85.85±0.15</u>	83.69±0.15	74.20±1.42	85.09±0.29	83.96±0.13	81.57±0.94	86.34±0.17
	Weighted-F1	<u>85.78±0.16</u>	83.61±0.15	73.66±1.59	85.06±0.29	83.92±0.15	81.56±0.92	86.31±0.17
Arxiv	Accuracy	<u>62.26±0.23</u>	>3days	23.60±7.63	48.13±0.48	61.19±0.33	OOM	63.52±0.12
	Weighted-F1	<u>60.54±0.25</u>	>3days	14.67±6.82	41.24±0.46	59.08±0.40	OOM	62.09±0.17

Table 4: Evaluation of tail node classification using other GNNs as the base model. "Acc." denotes accuracy(%) and "WF1." denotes weighted-f1 score (%). "OOM" denotes that the model runs out of memory.

	GAT		SAILOR		GraphSAGE		SAILOR	
	Acc. (%)	WF1. (%)	Acc. (%)	WF1. (%)	Acc. (%)	WF1. (%)	Acc. (%)	WF1. (%)
Chameleon	31.12±1.76	25.90±2.54	36.25±1.62	32.77±3.06	32.04±3.68	29.12±6.35	37.38±1.45	35.29±1.62
Squirrel	20.81±3.38	10.29±4.69	26.00±1.54	20.09±2.45	26.47±2.12	19.30±3.70	30.72±1.43	23.97±2.91
Cora	85.31±0.55	85.34±0.60	86.50±0.42	86.52±0.45	85.39±0.46	85.41±0.48	86.48±0.40	86.52±0.39
Citeseer	71.55±0.77	70.08±0.88	73.72±0.99	72.30±1.01	71.20±0.56	69.71±0.68	74.39±0.61	72.69±0.63
Pubmed	85.28±0.15	85.25±0.15	85.39±0.19	85.36±0.19	84.62±0.14	84.58±0.14	84.96±0.19	84.92±0.19
Arxiv	OOM	OOM	OOM	OOM	62.44±0.23	60.61±0.32	63.85±0.13	62.08±0.17

previous work [22, 23], while adhering to the standard definition, we adopt the Weighted-F1 score from sklearn.

We employ the well-established GCN as the base model for all the GNN-based approaches to ensure a fair comparison. To examine the generalizability of SAILOR for other GNN architectures, we also show how it performs on GAT and GraphSAGE.

Using GCN as the base model. Table 3 displays the tail node classification results. The superior performance of SAILOR demonstrates that it learns a more representative feature transformation pattern and extracts high-quality tail node representations. From these results, we can draw two conclusions. Firstly, SAILOR achieves state-of-the-art performance compared to existing tail node representation learning baselines, suggesting that jointly augmenting the graph structure and refining the node representations can enhance the model. Secondly, SAILOR outperforms GCN, its underlying GNN architecture, indicating that the pseudo-homophilic edges generated by the tail structure augmentor are useful and facilitate the training of the GNN.

Using other GNNs as base models. SAILOR is a versatile framework that can be applied to various GNNs. To validate this claim, we further implemented GAT and GraphSAGE within the framework and present their results in Table 4. These results also demonstrate the superiority of SAILOR over the vanilla GNN models.

6.3 Importance of Structure Augmentation

In this subsection, we aim to understand the augmented graph generated by the tail structure augmentor. Specifically, we calculate the homophily of all nodes in both the original and augmented graphs. The cumulative distribution of homophily for all nodes in both graphs is presented in Figure 6. The horizontal axis represents node homophily, while the vertical axis represents cumulative density, indicating the proportion of nodes with homophily values less than or equal to that value. From Figure 6, we observe that there are fewer total-heterophilic nodes in the augmented graph, demonstrating that SAILOR decreases the proportion of total-heterophilic nodes as expected. Additionally, the proportion of nodes with higher homophily values is larger in the augmented graph than in the original graph, confirming that the augmented graph facilitates GNN training by adding pseudo-homophilic edges to tail nodes.

6.4 Ablation Study and Parameter Analysis

We compare SAILOR with its four variants to examine the importance of different components. Specifically, we implement the following variants: (1) *SAILOR-w/o-Augm.*: We employ a vanilla VGAE to conduct neighbor generation and train it with the objective $\mathcal{L} = \gamma \mathcal{L}_{vgae} + \mathcal{L}_{sup}$, where \mathcal{L}_{vgae} is the well-established loss for vanilla VGAE and \mathcal{L}_{sup} is the semi-supervised node classification

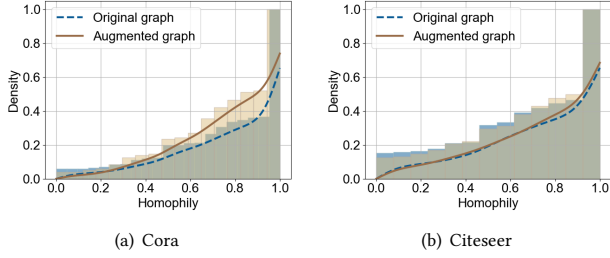


Figure 6: The cumulative distribution of homophily for all nodes in the original and augmented graphs, respectively.

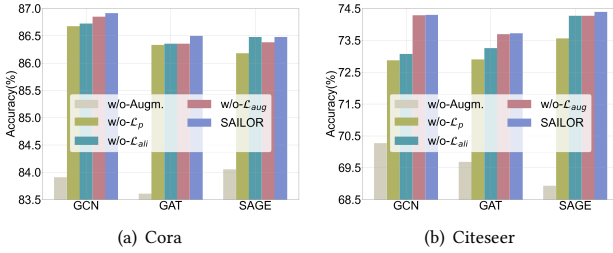


Figure 7: Node classification performance of SAILOR variants.

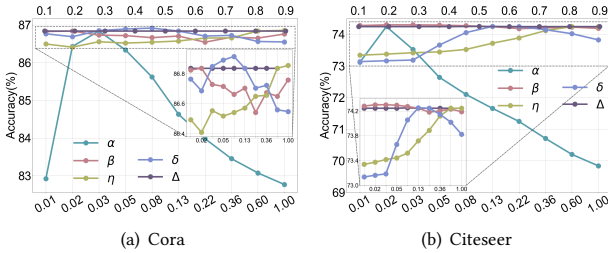


Figure 8: Parameter analysis on Cora and Citeseer. The lower horizontal axis represents the values of α , β , η , and θ , which are evenly spaced on a logarithmic scale from 0.01 to 1. The upper horizontal axis represents the values of Δ .

loss. We fine-tune γ for a fair comparison. (2) SAILOR-w/o- \mathcal{L}_{aug} : We remove the augmentation constraint for the tail structure augmentor by setting β to zero. (3) SAILOR-w/o- \mathcal{L}_p : We remove the propagation constraint for the tail structure augmentor by setting η to zero. (4) SAILOR-w/o- \mathcal{L}_{al} : We remove the alignment constraint for the tail structure augmentor by setting δ to zero.

The experiment results are shown in Figure 7, from which we can make several observations. Firstly, SAILOR-w/o- \mathcal{L}_{aug} performs significantly worse than all other variants, emphasizing the crucial role of the tail structure augmentor in enhancing the performance of SAILOR. Secondly, all three constraints contribute to the performance of SAILOR; removing any one of them results in a decrease in performance. This indicates that each constraint is necessary for achieving optimal performance.

Table 5: Node classification accuracy under public dataset partitioning setting as in [18].

Citeseer	Test	Head	Tail
GCN	68.29±0.65	75.42±0.52	67.00±0.78
DEMO-Net	65.48±1.20	72.35±1.75	64.24±1.41
Tail-GCN	69.18±1.04	77.78±1.65	67.63±1.01
Cold Brew	66.60±0.40	74.84±1.35	65.11±0.51
GRADE	68.92±1.37	68.81±4.61	68.93±1.35
SAILOR	73.91±0.74	80.39±2.09	72.74±0.96

We also explored the sensitivity of SAILOR to various hyper-parameters, including the loss weight of GNN (α), the three constraints for the tail structure augmentor (β , η , δ), and the edge-dropped proportion for converting head nodes into forged tail nodes (Δ). Experiments are performed by altering the value of each hyper-parameter while keeping the others fixed. GCN is used as the base architecture for these experiments. The results, reported in Figure 8, show that changes in the weight of GNN (α) can significantly affect the performance of SAILOR. There is an optimal value for α , and deviating from this value can impair performance. In contrast, the performance of SAILOR is generally insensitive to changes in β , η , δ , and Δ , with performance changes of only about one percentage point at most as their values vary.

6.5 Tail Node Classification under Public Split

In this subsection, we align the dataset partition setting with that of GCN [18] to further confirm the effectiveness of SAILOR. The experiment results, reported in Table 5, show that SAILOR still achieves superior performance in tail node classification under public partitioning setting as in [18]. Besides, the results indicate that the performance of head nodes has also been significantly improved. This is because we process the edges in the graph as undirected. When the tail structure augmentor adds pseudo-homophilic edges to tail nodes, it may also add pseudo-homophilic edges to some head nodes. This can enhance the structural information of head nodes and promotes their representation learning.

7 CONCLUSION

In this paper, we focus on the problem of tail node representation learning and propose a general structural augmentation based method, SAILOR. We find that the lack of structural information in tail nodes is a contributing factor to total-heterophily, which significantly impairs GNNs' performance. To tackle this problem, SAILOR exploits a tail structure augmentor with three well-designed constraint strategies to add pseudo-homophilic edges to tail nodes. This decreases the ratio of total-heterophilic nodes in the graph, thereby facilitating the training of GNNs. Extensive experiments on public datasets demonstrate the effectiveness of SAILOR.

ACKNOWLEDGMENTS

The research is supported by the National Key R&D Program of China under grant No. 2022YFF0902500, the Guangdong Basic and Applied Basic Research Foundation, China (No. 2023A1515011050), the Tencent AI Lab RBFR2022017.

REFERENCES

- [1] Deli Chen, Yankai Lin, Wei Li, Peng Li, Jie Zhou, and Xu Sun. 2020. Measuring and Relieving the Over-Smoothing Problem for Graph Neural Networks from the Topological View. In *The Thirty-Fourth AAAI Conference on Artificial Intelligence, AAAI 2020, The Thirty-Second Innovative Applications of Artificial Intelligence Conference, IAAI 2020, The Tenth AAAI Symposium on Educational Advances in Artificial Intelligence, EAAI 2020*, New York, NY, USA, February 7–12, 2020. AAAI Press, 3438–3445. <https://ojs.aaai.org/index.php/AAAI/article/view/5747>
- [2] Liang Chen, Jintang Li, Jiaying Peng, Tao Xie, Zengxu Cao, Kun Xu, Xiangnan He, and Zibin Zheng. 2020. A Survey of Adversarial Learning on Graphs. *CoRR* abs/2003.05730 (2020). arXiv:2003.05730 <https://arxiv.org/abs/2003.05730>
- [3] Liang Chen, Yang Liu, Xiangnan He, Lianli Gao, and Zibin Zheng. 2019. Matching User with Item Set: Collaborative Bundle Recommendation with Deep Attention Network. In *Proceedings of the Twenty-Eighth International Joint Conference on Artificial Intelligence, IJCAI 2019, Macao, China, August 10–16, 2019*, Sarit Kraus (Ed.), ijcai.org, 2095–2101. <https://doi.org/10.24963/ijcai.2019/290>
- [4] Wei-Lin Chiang, Xuanqing Liu, Si Si, Yang Li, Samy Bengio, and Cho-Jui Hsieh. 2019. Cluster-GCN: An Efficient Algorithm for Training Deep and Large Graph Convolutional Networks. In *Proceedings of the 25th ACM SIGKDD International Conference on Knowledge Discovery & Data Mining (KDD '19)*. ACM, New York, NY, USA, 257–266. <https://doi.org/10.1145/3292500.3330925>
- [5] Eli Chien, Jianhao Peng, Pan Li, and Olga Milenkovic. 2021. Adaptive Universal Generalized PageRank Graph Neural Network. In *9th International Conference on Learning Representations, ICLR 2021, Virtual Event, Austria, May 3–7, 2021*. OpenReview.net. <https://openreview.net/forum?id=n6jl7LxRP>
- [6] Kaize Ding, Zhe Xu, Hanghang Tong, and Huan Liu. 2022. Data Augmentation for Deep Graph Learning: A Survey. *SIGKDD Explor. NewsL* 24, 2 (dec 2022), 61–77. <https://doi.org/10.1145/3575637.3575646>
- [7] Chelsea Finn, Pieter Abbeel, and Sergey Levine. 2017. Model-Agnostic Meta-Learning for Fast Adaptation of Deep Networks. In *Proceedings of the 34th International Conference on Machine Learning, ICML 2017, Sydney, NSW, Australia, 6–11 August 2017 (Proceedings of Machine Learning Research, Vol. 70)*, Doina Precup and Yee Whye Teh (Eds.), PMLR, 1126–1135. <http://proceedings.mlr.press/v70/finn17a.html>
- [8] Joseph E. Gonzalez, Reynold S. Xin, Ankur Dave, Daniel Crankshaw, Michael J. Franklin, and Ion Stoica. 2014. GraphX: Graph Processing in a Distributed Dataflow Framework. In *Proceedings of the 11th USENIX Conference on Operating Systems Design and Implementation (OSDI'14)*. USENIX Association, USA, 599–613.
- [9] Ian J. Goodfellow, Jean Pouget-Abadie, Mehdi Mirza, Bing Xu, David Warde-Farley, Sherjil Ozair, Aaron C. Courville, and Yoshua Bengio. 2014. Generative Adversarial Nets. In *Advances in Neural Information Processing Systems 27: Annual Conference on Neural Information Processing Systems 2014, December 8–13 2014, Montreal, Quebec, Canada*, Zoubin Ghahramani, Max Welling, Corinna Cortes, Neil D. Lawrence, and Kilian Q. Weinberger (Eds.), 2672–2680. <https://proceedings.neurips.cc/paper/2014/hash/5ca3e9b122f61f8f06494c97b1afcc3-Abstract.html>
- [10] Daniel Gruhl, R. Guha, David Liben-Nowell, and Andrew Tomkins. 2004. Information Diffusion through Blogspace. In *Proceedings of the 13th International Conference on World Wide Web (WWW '04)*. ACM, New York, NY, USA, 491–501. <https://doi.org/10.1145/988672.988739>
- [11] William L. Hamilton, Zhitao Ying, and Jure Leskovec. 2017. Inductive Representation Learning on Large Graphs. In *Advances in Neural Information Processing Systems 30: Annual Conference on Neural Information Processing Systems 2017, December 4–9, 2017, Long Beach, CA, USA*, Isabelle Guyon, Ulrike von Luxburg, Samy Bengio, Hanna M. Wallach, Rob Fergus, S. V. N. Vishwanathan, and Roman Garnett (Eds.), 1024–1034. <https://proceedings.neurips.cc/paper/2017/hash/5dd9db5e033da9c6fb5ba83c7a7e9ea9-Abstract.html>
- [12] John R. Hershey and Peder A. Olsen. 2007. Approximating the Kullback Leibler Divergence Between Gaussian Mixture Models. In *Proceedings of the IEEE International Conference on Acoustics, Speech, and Signal Processing, ICASSP 2007, Honolulu, Hawaii, USA, April 15–20, 2007*. IEEE, 317–320. <https://doi.org/10.1109/ICASSP.2007.366913>
- [13] Yifan Hou, Jian Zhang, James Cheng, Kaili Ma, Richard T. B. Ma, Hongzhi Chen, and Ming-Chang Yang. 2020. Measuring and Improving the Use of Graph Information in Graph Neural Networks. In *8th International Conference on Learning Representations, ICLR 2020, Addis Ababa, Ethiopia, April 26–30, 2020*. OpenReview.net. <https://openreview.net/forum?id=rkelkHKvS>
- [14] Weihua Hu, Matthias Fey, Marinka Zitnik, Yuxiao Dong, Hongyu Ren, Bowen Liu, Michele Catasta, and Jure Leskovec. 2020. Open Graph Benchmark: Datasets for Machine Learning on Graphs. In *Advances in Neural Information Processing Systems 33: Annual Conference on Neural Information Processing Systems 2020, NeurIPS 2020, December 6–12, 2020, virtual*, Hugo Larochelle, Marc'Aurelio Ranzato, Raia Hadsell, Maria-Florina Balcan, and Hsuan-Tien Lin (Eds.), <https://proceedings.neurips.cc/paper/2020/hash/fb60d411a5c5b72b2e7d3527cfc84fd0-Abstract.html>
- [15] Wei Jin, Yao Ma, Xiaorui Liu, Xianfeng Tang, Suhang Wang, and Jiliang Tang. 2020. Graph Structure Learning for Robust Graph Neural Networks. In *Proceedings of the 26th ACM SIGKDD International Conference on Knowledge Discovery & Data Mining (KDD '20)*. ACM, New York, NY, USA, 66–74. <https://doi.org/10.1145/3394486.3403049>
- [16] Diederik P. Kingma and Max Welling. 2014. Auto-Encoding Variational Bayes. In *2nd International Conference on Learning Representations, ICLR 2014, Banff, AB, Canada, April 14–16, 2014, Conference Track Proceedings*, Yoshua Bengio and Yann LeCun (Eds.). <http://arxiv.org/abs/1312.6114>
- [17] Thomas N. Kipf and Max Welling. 2016. Variational Graph Auto-Encoders. *CoRR* abs/1611.07308 (2016). arXiv:1611.07308 <http://arxiv.org/abs/1611.07308>
- [18] Thomas N. Kipf and Max Welling. 2017. Semi-Supervised Classification with Graph Convolutional Networks. In *5th International Conference on Learning Representations, ICLR 2017, Toulon, France, April 24–26, 2017, Conference Track Proceedings*. OpenReview.net. <https://openreview.net/forum?id=SJU4ayYgl>
- [19] Haewoon Kwak, Changhyun Lee, Hosung Park, and Sue Moon. 2010. What is Twitter, a Social Network or a News Media?. In *Proceedings of the 19th International Conference on World Wide Web (WWW '10)*. ACM, New York, NY, USA, 591–600. <https://doi.org/10.1145/1772690.1772751>
- [20] Jure Leskovec, Jon Kleinberg, and Christos Faloutsos. 2007. Graph Evolution: Densification and Shrinking Diameters. *ACM Trans. Knowl. Data Eng.* 1, 1 (mar 2007), 2–es. <https://doi.org/10.1145/1217299.1217301>
- [21] Jintang Li, Tao Xie, Liang Chen, Fenfang Xie, Xiangnan He, and Zibin Zheng. 2023. Adversarial Attack on Large Scale Graph. *IEEE Trans. Knowl. Data Eng.* 35, 1 (2023), 82–95. <https://doi.org/10.1109/TKDE.2021.3078755>
- [22] Zemin Liu, Trung-Kien Nguyen, and Yuan Fang. 2021. Tail-GNN: Tail-Node Graph Neural Networks. In *Proceedings of the 27th ACM SIGKDD Conference on Knowledge Discovery & Data Mining (KDD '21)*. ACM, New York, NY, USA, 1109–1119. <https://doi.org/10.1145/3447548.3467276>
- [23] Zemin Liu, Wentao Zhang, Yuan Fang, Xinming Zhang, and Steven C.H. Hoi. 2020. Towards Locality-Aware Meta-Learning of Tail Node Embeddings on Networks. In *Proceedings of the 29th ACM International Conference on Information & Knowledge Management (CIKM '20)*. ACM, New York, NY, USA, 975–984. <https://doi.org/10.1145/3340531.3411910>
- [24] Yucheng Low, Danny Bickson, Joseph Gonzalez, Carlos Guestrin, Aapo Kyrola, and Joseph M. Hellerstein. 2012. Distributed GraphLab: A Framework for Machine Learning and Data Mining in the Cloud. *Proc. VLDB Endow.* 5, 8 (apr 2012), 716–727. <https://doi.org/10.14778/2212351.2212354>
- [25] Yunshan Ma, Yingzhi He, An Zhang, Xiang Wang, and Tat-Seng Chua. 2022. CrossCBR: Cross-View Contrastive Learning for Bundle Recommendation. In *Proceedings of the 28th ACM SIGKDD Conference on Knowledge Discovery and Data Mining (KDD '22)*. ACM, New York, NY, USA, 1233–1241. <https://doi.org/10.1145/3534678.3539229>
- [26] Julian McAuley, Christopher Targett, Qinfeng Shi, and Anton van den Hengel. 2015. Image-Based Recommendations on Styles and Substitutes. In *Proceedings of the 38th International ACM SIGIR Conference on Research and Development in Information Retrieval (SIGIR '15)*. ACM, New York, NY, USA, 43–52. <https://doi.org/10.1145/2766462.2767755>
- [27] Péter Mernyei and Catalina Cangea. 2020. Wiki-CS: A Wikipedia-Based Benchmark for Graph Neural Networks. *CoRR* abs/2007.02901 (2020). arXiv:2007.02901 <https://arxiv.org/abs/2007.02901>
- [28] Alan Mislove, Massimiliano Marcon, Krishna P. Gummadi, Peter Druschel, and Bobby Bhattacharjee. 2007. Measurement and Analysis of Online Social Networks. In *Proceedings of the 7th ACM SIGCOMM Conference on Internet Measurement (IMC '07)*. ACM, New York, NY, USA, 29–42. <https://doi.org/10.1145/1298306.1298311>
- [29] Hongbin Pei, Bingzhe Wei, Kevin Chen-Chuan Chang, Yu Lei, and Bo Yang. 2020. Geom-GCN: Geometric Graph Convolutional Networks. In *8th International Conference on Learning Representations, ICLR 2020, Addis Ababa, Ethiopia, April 26–30, 2020*. OpenReview.net. <https://openreview.net/forum?id=S1e2agrFvS>
- [30] Benedek Rozemberczki, Carl Allen, and Rik Sarkar. 2021. Multi-Scale attributed node embedding. *J. Complex Networks* 9, 2 (2021). <https://doi.org/10.1093/comnet/cnab014>
- [31] Robert Sanders. 1987. The Pareto principle: its use and abuse. *Journal of Services Marketing* 1, 2 (1987), 37–40.
- [32] Prithviraj Sen, Galileo Namata, Mustafa Bilgic, Lise Getoor, Brian Gallagher, and Tina Eliassi-Rad. 2008. Collective Classification in Network Data. *AI Mag.* 29, 3 (2008), 93–106. <https://doi.org/10.1609/aimag.v29i3.2157>
- [33] Xianfeng Tang, Huaxiu Yao, Yiwei Sun, Yiqi Wang, Jiliang Tang, Charu Aggarwal, Prasenjit Mitra, and Suhang Wang. 2020. Investigating and Mitigating Degree-Related Biases in Graph Convolutional Networks. In *Proceedings of the 29th ACM International Conference on Information & Knowledge Management (CIKM '20)*. ACM, New York, NY, USA, 1435–1444. <https://doi.org/10.1145/3340531.3411872>
- [34] Cunchao Tu, Xiangkai Zeng, Hao Wang, Zhengyan Zhang, Zhiyuan Liu, Maosong Sun, Bo Zhang, and Leyu Lin. 2019. A Unified Framework for Community Detection and Network Representation Learning. *IEEE Trans. Knowl. Data Eng.* 31, 6 (2019), 1051–1065. <https://doi.org/10.1109/TKDE.2018.2852958>
- [35] Petar Velickovic, Guillem Cucurull, Arantxa Casanova, Adriana Romero, Pietro Liò, and Yoshua Bengio. 2018. Graph Attention Networks. In *6th International Conference on Learning Representations, ICLR 2018, Vancouver, BC, Canada, April 30 – May 3, 2018, Conference Track Proceedings*. OpenReview.net. <https://openreview.net/forum?id=rJXMpikCZ>

- [36] Ruijia Wang, Xiao Wang, Chuan Shi, and Le Song. 2022. Uncovering the Structural Fairness in Graph Contrastive Learning. In *NeurIPS*. http://papers.nips.cc/paper_files/paper/2022/hash/d13565c82d1e44eda2da3bd00b35ca11-Abstract-Conference.html
- [37] Xiao Wang, Meiqi Zhu, Deyu Bo, Peng Cui, Chuan Shi, and Jian Pei. 2020. AM-GCN: Adaptive Multi-Channel Graph Convolutional Networks. In *Proceedings of the 26th ACM SIGKDD International Conference on Knowledge Discovery & Data Mining (KDD '20)*. ACM, New York, NY, USA, 1243–1253. <https://doi.org/10.1145/3394486.3403177>
- [38] Jun Wu, Jingrui He, and Jiejun Xu. 2019. DEMO-Net: Degree-Specific Graph Neural Networks for Node and Graph Classification. In *Proceedings of the 25th ACM SIGKDD International Conference on Knowledge Discovery & Data Mining (KDD '19)*. ACM, New York, NY, USA, 406–415. <https://doi.org/10.1145/3292500.3330950>
- [39] Keyulu Xu, Chengtao Li, Yonglong Tian, Tomohiro Sonobe, Ken-ichi Kawarabayashi, and Stefanie Jegelka. 2018. Representation Learning on Graphs with Jumping Knowledge Networks. In *Proceedings of the 35th International Conference on Machine Learning, ICML 2018, Stockholmsmässan, Stockholm, Sweden, July 10-15, 2018 (Proceedings of Machine Learning Research, Vol. 80)*, Jennifer G. Dy and Andreas Krause (Eds.). PMLR, 5449–5458. <http://proceedings.mlr.press/v80/xu18c.html>
- [40] Yuan Zhang, Tianshu Lyu, and Yan Zhang. 2018. COSINE: Community-Preserving Social Network Embedding From Information Diffusion Cascades. In *Proceedings of the Thirty-Second AAAI Conference on Artificial Intelligence, (AAAI-18), the 30th innovative Applications of Artificial Intelligence (IAAI-18), and the 8th AAAI Symposium on Educational Advances in Artificial Intelligence (EAAI-18)*, New Orleans, Louisiana, USA, February 2-7, 2018, Sheila A. McIlraith and Kilian Q. Weinberger (Eds.). AAAI Press, 2620–2627. <https://www.aaai.org/ocs/index.php/AAAI/AAAI18/paper/view/16364>
- [41] Tong Zhao, Yozen Liu, Leonardo Neves, Oliver J. Woodford, Meng Jiang, and Neil Shah. 2021. Data Augmentation for Graph Neural Networks. In *Thirty-Fifth AAAI Conference on Artificial Intelligence, AAAI 2021, Thirty-Third Conference on Innovative Applications of Artificial Intelligence, IAAI 2021, The Eleventh Symposium on Educational Advances in Artificial Intelligence, EAAI 2021, Virtual Event, February 2-9, 2021*. AAAI Press, 11015–11023. <https://ojs.aaai.org/index.php/AAAI/article/view/17315>
- [42] Wenqing Zheng, Edward W. Huang, Nikhil Rao, Sumeet Katariya, Zhangyang Wang, and Karthik Subbian. 2022. Cold Brew: Distilling Graph Node Representations with Incomplete or Missing Neighborhoods. In *The Tenth International Conference on Learning Representations, ICLR 2022, Virtual Event, April 25-29, 2022*. OpenReview.net. <https://openreview.net/forum?id=1ugNpm7W6E>
- [43] Jiong Zhu, Yujun Yan, Lingxiao Zhao, Mark Heimann, Leman Akoglu, and Danai Koutra. 2020. Beyond Homophily in Graph Neural Networks: Current Limitations and Effective Designs. In *Advances in Neural Information Processing Systems 33: Annual Conference on Neural Information Processing Systems 2020, NeurIPS 2020, December 6-12, 2020, virtual*, Hugo Larochelle, Marc'Aurelio Ranzato, Raia Hadsell, Maria-Florina Balcan, and Hsuan-Tien Lin (Eds.). <https://proceedings.neurips.cc/paper/2020/hash/58ae23d878a47004366189884c2f8440-Abstract.html>